

Attachment and Detachment Behavior of Human Adenovirus and Surrogates in Fine Granular Limestone Aquifer Material

Margaret E. Stevenson,* Regina Sommer, Gerhard Lindner, Andreas H. Farnleitner, Simon Toze, Alexander K.T. Kirschner, Alfred P. Blaschke, Jatinder P.S. Sidhu

Abstract

The transport of human adenovirus, nanoparticles, and PRD1 and MS2 bacteriophages was tested in fine granular limestone aquifer material taken from a borehole at a managed aquifer recharge site in Adelaide, South Australia. Comparison of transport and removal of virus surrogates with the pathogenic virus is necessary to understand the differences between the virus and surrogate. Because experiments using pathogenic viruses cannot be done in the field, laboratory tests using flow-through soil columns were used. Results show that PRD1 is the most appropriate surrogate for adenovirus in an aquifer dominated by calcite material but not under high ionic strength or high pH conditions. It was also found that straining due to size and the charge of the colloid were not dominant removal mechanisms in this system. Implications of this study indicate that a certain surrogate may not represent a specific pathogen solely based on similar size, morphology, and/or surface charge. Moreover, if a particular surrogate is representative of a pathogen in one aquifer system, it may not be the most appropriate surrogate in another porous media system. This was apparent in the inferior performance of MS2 as a surrogate, which is commonly used in virus transport studies.

Core Ideas

- Adenovirus was compared to three surrogates: 100-nm particles and MS2 and PRD1 bacteriophages.
- Column tests were performed in experiments using fine granular limestone aquifer material.
- Column experiments under variable chemical conditions have not been done before using adenovirus.
- PRD1 bacteriophage was the best surrogate to model the attachment of adenovirus but not detachment.
- Implications of the work could influence interpretation of experiments using surrogates.

ARTIFICIAL stormwater recharge, or managed aquifer recharge (MAR), has become a popular potential drinking water resource in many countries due to its successful attenuation of pathogens and other substances in the subsurface and the subsequent possible decrease of drinking water treatment costs. Most MAR projects, however, are still in the feasibility stage, usually involving a Quantitative Microbial Risk Assessment, and quantitative experiments demonstrating the efficacy of removal are required. One such project is the Salisbury stormwater recharge project near Adelaide, South Australia.

A quantitative study of virus transport and removal in aquifer material in the laboratory is a useful first step to investigating field studies. This study compared the transport of human adenovirus (HAdV), a common virus that causes childhood diarrhea, in small columns of fine granular limestone with three different virus surrogates: PRD1 and MS2 bacteriophages and 100-nm carboxylated polystyrene nanoparticles. This was done to assess the suitability of the surrogates for further investigations, possibly in the field, and to establish preliminary attachment and detachment rates for the colloids in the aquifer material, as well as defining a preliminary removal rate.

Human adenovirus from human fecal sources is present in surface water and groundwater, but its transport in groundwater has not yet been widely studied. Prevalent in urban stormwater runoff (Sidhu et al., 2012), HAdV was also detected in a large river and its watershed (Corsi et al., 2014) and has been found in groundwater (Futch et al., 2010), possibly leaking into the subsurface from sewage pipes (Bradbury et al., 2013). Because of its resistance to treatment such as chlorination and ultraviolet disinfection (Calgua et al., 2014; Rodriguez et al., 2008) and its persistence in sewage and treated water with a very long

Copyright © 2015 American Society of Agronomy, Crop Science Society of America, and Soil Science Society of America. 5585 Guilford Rd., Madison, WI 53711 USA. All rights reserved.

J. Environ. Qual. 44:1392–1401 (2015)

doi:10.2134/jeq2015.01.0052

Freely available online through the author-supported open-access option.

Received 30 Jan. 2015.

Accepted 26 May 2015.

*Corresponding author (stevenson@waterresources.at).

M.E. Stevenson, Centre for Water Resource Systems, Vienna Univ. of Technology, Karlsplatz 13, A-1040 Vienna, Austria; M.E. Stevenson, R. Sommer, G. Lindner, A.H. Farnleitner, A.K.T. Kirschner, and A.P. Blaschke, Interuniversity Cooperation Centre Water and Health (ICC), www.waterandhealth.at; R. Sommer, G. Lindner, and A.K.T. Kirschner, Institute for Hygiene and Applied Immunology, Medical Univ. of Vienna, Kinderspitalgasse 15, A-1090 Vienna, Austria; A.H. Farnleitner, Institute of Chemical Engineering, Research Group Environmental Microbiology and Molecular Ecology, Vienna Univ. of Technology, Gumpendorfer Straße 1a, A-1060 Vienna, Austria; S. Toze and J.P.S. Sidhu, CSIRO Land and Water Flagship, Ecosciences Precinct, 41 Boggo Road, 4102 Brisbane, QLD, Australia; and A.P. Blaschke, Institute of Hydraulic Engineering and Water Resources Management, Vienna Univ. of Technology, Karlsplatz 13, A-1040 Vienna, Austria. Assigned to Associate Editor Jack Schijven.

Abbreviations: DI, deionized; HAdV, human adenovirus; IS, ionic strength; MAR, managed aquifer recharge; qPCR, quantitative polymerase chain reaction.

survival time, HAdV is a conservative pathogenic microorganism. A study in Barcelona, Spain, tested samples of effluent from a drinking water treatment plant next to the Llobregat River and found a 2 log₁₀ removal (two orders of magnitude decrease) of HAdV compared with the raw influent water; however, low concentrations of HAdV were still detected, whereas fecal bacterial indicators were no longer detected (Albinana-Gimenez et al., 2006). Due to the persistence of HAdV, it can be used as an appropriate fecal indicator (Ahmed et al., 2010; Bofill-Mas et al., 2006). Although HAdV is present in the environment and demonstrates a higher resistance to environmental factors, few groundwater column test studies have been done using HAdV.

The PRD1 bacteriophage has been mentioned in groundwater studies as being a potential surrogate for rotavirus and HAdV (Harvey and Ryan, 2004; Sadeghi et al., 2013; Sinton et al., 1997). Mesquita et al. (2010) suggested that PRD1 may be the best available surrogate for pathogenic HAdV because of its size, structural similarity to HAdV, and its long survival time in the environment. It has been found to be very persistent in soil at ambient temperature (Blanc and Nasser, 1996) and could be a suitable surrogate for HAdV, which also has a very low inactivation rate in the subsurface environment (Sidhu et al., 2010). PRD1 has even been shown to be more conservative than HAdV, exhibiting lower inactivation rates in soil (Davies et al., 2006). Harvey and Ryan (2004), in a mini-review on the application of PRD1 in colloidal transport studies, listed the many groundwater transport tests in the field as well as in the laboratory that have used PRD1. Transport studies in a limestone aquifer in the Florida Keys used PRD1 as a virus surrogate and found surprisingly fast travel times in the highly porous limestone bedrock, emphasizing the vulnerability of limestone aquifers to viral contamination (Paul et al., 1995, 1997).

The MS2 bacteriophage is widely used as a surrogate for virus transport in groundwater because it is considered a conservative surrogate (i.e., it often overpredicts breakthrough [Schijven et al., 2003], adding a safety factor) and it is of a similar size to many enteroviruses. Transport of MS2 has also been compared with that of nanoparticles. The MS2 and PR772 phages were compared with 20- and 200-nm carboxylated latex nanoparticles in fractured dolomite laboratory-scale tests (Mondal and Sleep, 2013). The retention of MS2 was found to be lower than the retention of similarly sized 20-nm nanoparticles.

Carboxylated polystyrene nanoparticles are commonly used as surrogates to mimic transport of pathogenic microorganisms in groundwater experiments in the field (Bales et al., 1997) and in the laboratory (Tufenkji et al., 2004). Pang et al. (2009) developed protein-coated 20-nm polystyrene nanoparticles to better mimic the transport of viruses in groundwater due to the similar surface charge of the protein-coated particles compared with the viruses.

Column tests in the laboratory using active viruses are not common because working with pathogenic microorganisms is more complicated and requires work in a biological safety laboratory. For this reason, it is not as common to perform column tests with the real pathogen in question. Several studies have done column tests to investigate the transport of viruses in groundwater to compare with the transport of corresponding surrogates. Hepatitis A, poliovirus, echovirus, coxsackievirus, and Norwalk virus have all been compared with MS2 in column tests. Sobsey

et al. (1995) compared the retention of MS2 to that of hepatitis A, poliovirus 1, and echovirus 1 in small (10-cm) soil columns. Schijven et al. (2003) performed the first study showing the complete breakthrough curve of pathogenic viruses (coxsackievirus B4 and poliovirus 1) and compared the transport of these viruses with MS2. Even though poliovirus and MS2 are similar in size, there was a difference of 4 log₁₀ removal in the column tests, MS2 being more conservative and breaking through with very little or no removal. In contrast to poliovirus, coxsackievirus, which is also close in size to MS2, had removal similar to MS2. Redman et al. (1997) compared recombinant Norwalk virus (non-infectious) to MS2 and concluded that MS2 is not a good surrogate for Norwalk virus because their electrostatic properties differ, although they are of similar size and shape. To the best of our knowledge, very little attention has been given to HAdV in flow-through column experiments until recently (Kokkinos et al., 2015; Pang et al., 2014; Wong et al., 2014), and, to date, there have not been any column tests in material taken from a deep aquifer or detachment tests under variable chemical conditions using HAdV.

The intention of this study was to determine the best surrogate for HAdV, and we considered three possible surrogates: PRD1, MS2, and 100-nm carboxylated polystyrene particles. The surrogates were chosen to test the influence of size, morphology, and surface charge on groundwater transport. Human adenovirus Type 41 has an icosahedral structure and a size of 68 nm (Pang et al., 2014) and is similar in structure and size to PRD1, which is icosahedral and 62 nm in diameter (Ryan et al., 1999). MS2, which is 26 nm in diameter (Pang et al., 2009), is also icosahedral, and its surface charge is potentially the most similar to that of HAdV. Human adenovirus is similar in size to, although slightly smaller than, the spherical 100-nm nanoparticles, but the icosahedral structure is not shared, nor is the surface charge thought to be similar. By testing these three surrogates in particular, we wanted to determine which mechanism is important for the removal of HAdV, for example, straining or electrostatic interactions. The other goal of our study was to observe the detachment of HAdV under high ionic strength (IS) and high pH conditions and to see if a surrogate, such as PRD1, would also detach in a similar manner.

Materials and Methods

Porous Medium

The aquifer material was collected from a MAR site in Parafield Gardens, Adelaide, SA, Australia (for more details, see Stevenson et al., 2015). The tertiary limestone aquifer consists of fine granular limestone with some consolidated chunks. Aquifer material was obtained from core samples taken at a depth of between 170 and 180 m below ground surface. The core material was rinsed in deionized (DI) water and baked in an oven overnight at 80°C before sieve analysis. The material used in the soil column had a grain size of 150 to 250 μm with a median grain size of 200 μm.

Standard gravimetric methods were used to determine the effective porosity. Calculated from the amount of water and material packed in each column, the effective porosity was 0.46 ± 0.001 and the bulk density was 1.31 ± 0.003 g cm⁻³.

The aquifer material consisted mainly of calcite (63%) and quartz (31.3%), with other minerals including microcline (1.6%), aragonite (1.5%), albite (0.7%), goethite (0.6%), pyrite (0.5%), ankerite (0.4%), and hematite (0.3%). Geochemical analysis of the material was done by X-ray diffraction analysis.

Column Experiments

The columns were wet-packed in 0.5-cm lifts, while being gently tapped along the side, and were packed with fresh material for each replicate test. Ten-centimeter-long glass chromatography columns were used with an internal diameter of 1.5 cm. A flow rate of $1.26 \pm 0.19 \text{ m d}^{-1}$, mimicking the average flow rate in the aquifer, was injected at the top of the saturated column using a peristaltic pump (Masterflex), and the effluent was collected in test tubes at the outflow point at the bottom of the column. At least 50 pore volumes were pumped through the column before tests were begun to equilibrate the chemical conditions of the column. This was done so that the average pH between the influent and effluent solutions did not go above 8.3. The pH of the influent and effluent differed from the average by ± 0.5 . This was due to the constant leaching of carbonate during the column tests as a result of the high amount of carbonate minerals (calcite and aragonite) present in the aquifer material. The considerable variation of effluent pH observed (8.0–8.8 for the seven column tests; see Table 1) reflects the intrinsic variability of the amount of calcite and aragonite present in the material used for each column test.

The influent solution consisted of a $10 \text{ mmol L}^{-1} \text{ NaCl}$ solution, buffered to a pH of 8.0 ± 0.2 with NaHCO_3 . A small amount of Ca ($0.5 \text{ mmol L}^{-1} \text{ Ca}^{2+}$ as CaCl_2) was used in Run 1 with HAdV, with an overall solution IS of 10 mmol L^{-1} , to see if there was any effect from the Ca. The water temperature was kept at room temperature ($22\text{--}23^\circ\text{C}$) because the groundwater in the aquifer is 23°C at a depth of 160 to 180 m (Dillon et al., 2008).

Conservative tracer tests were done with $1 \text{ mmol L}^{-1} \text{ NaNO}_3$, and the effluent concentration of NO_3^- was measured by ultraviolet light absorption of NO_3^- ions by means of a UV-Vis spectrophotometer (Cary Series UV-Vis, Agilent Technologies) at a wavelength of 210 nm. Nitrate tests were performed

before HAdV and PRD1 tests (but in the same packed columns) because the UV-Vis spectrophotometer was outside of the quarantine area for pathogenic microorganisms, and samples to be analyzed could not contain any pathogenic viruses. Forty milliliters (approximately 4.8 pore volumes) of the tracer solution was injected for each test.

For the detachment portion of the experiment, first 10 mL of DI water (buffered to a pH of 7.0) was pumped through the column (approximately 1.2 pore volumes), followed by 10 mL of a solution high in pH and IS, followed again by 10 mL of DI water. The high-pH, high-IS solution used was 50 mmol L^{-1} glycine and 1.5% beef extract with a pH of 10.

Colloidal Particles

Human adenovirus Strain 41 (ATCC VR-930) was cultured in LLC-MK2 (rhesus monkey kidney) cell line by the Pathology Centre, Western Australia. The virus was then harvested and frozen at -80°C until further use. PRD1 (ATCC 19585-B2; somatic, double-stranded DNA virus, Tectiviridae) was cultured on an *Escherichia coli* (ATCC 11775) host. MS2 (NCTC 12487; F-specific, single-stranded RNA virus, Leviviridae) and host bacterium *E. coli* K-12 Hfr (NCTC 12486) were obtained from the National Collection of Type Cultures (London). The propagation was performed according to methods of the International Organization for Standardization (1995). Before using the phage stock suspension for the column experiments, it was filtered through a $0.2\text{-}\mu\text{m}$ membrane (Millex-GV, Millipore).

Yellow-green fluorescent carboxylated polystyrene nanoparticles (Fluoresbrite), with a diameter of 100 nm, were purchased from Polysciences Inc. These nanoparticles or microspheres are commonly used for microbial transport studies in groundwater (Knappett et al., 2008) due to their similarity in size and shape to pathogenic microorganisms and their strong fluorescent intensity.

Zeta Potential

The zeta potential of the porous medium was measured using a SurPASS electrokinetic analyzer (Anton Paar) based on a streaming potential and streaming current measurement (Luong

Table 1. Summary of measured experimental conditions: peak concentration (C_{max}), injection concentration (C_0), pulse duration (T_0), influent pH (pH_{in}), and effluent pH (pH_{out}).

Colloid	Run	Measured flow rate	C_{max}	C_0	C_{max}/C_0	$\log_{10}(C_{\text{max}}/C_0)$	T_0	pH_{in}	pH_{out}
		m d^{-1}	— pfu† mL^{-1} or n mL^{-1} —				min		
HAdV‡	1§	1.2	1.61×10^4	3.29×10^7	4.89×10^{-4}	-3.31	175	8.0	8.0
HAdV‡	2	1.2	1.45×10^4	4.59×10^7	3.15×10^{-4}	-3.50	220	7.9	8.7
HAdV‡	3	1.2	2.26×10^3	3.36×10^7	6.73×10^{-5}	-4.17	210	7.8	8.8
PRD1‡	2	1.2	6.10×10^3	2.40×10^8	2.54×10^{-5}	-4.59	220	7.9	8.7
PRD1‡	3	1.2	1.69×10^5	2.77×10^9	6.10×10^{-5}	-4.21	210	7.8	8.8
MS2¶	4	1.4	2.05×10^3	2.15×10^7	9.51×10^{-5}	-4.02	250	8.1	8.1
MS2¶	5	1.8	5.80×10^1	1.44×10^7	4.03×10^{-6}	-5.39	200	8.0	8.1
100 nm#	6	1.2	2.26×10^2	3.33×10^7	6.79×10^{-6}	-5.17	240	7.9	8.0
100 nm#	7	1.0	2.00×10^1	1.25×10^9	1.60×10^{-8}	-7.80	288	8.2	8.5

† pfu, plaque-forming units.

‡ Counted by quantitative polymerase chain reaction.

§ Included $0.5 \text{ mmol L}^{-1} \text{ Ca}^{2+}$.

¶ Counted by plaque assay.

#Counted by epifluorescence microscope.

and Sprik, 2013). The zeta potential measured by the analyzer is related to the surface charge at a solid–liquid interface.

Colloidal particles were tested with an electrophoretic light scattering device (Zetasizer Nano ZS, Malvern Instruments Ltd.), and all measurements were performed at least in triplicate. The zeta potential measurements for both the colloidal particles and the aquifer medium were done in a solution of 10 mmol L⁻¹ NaCl, buffered to a pH of 8.0 ± 0.2.

Enumeration of Colloidal Particles

Quantitative polymerase chain reaction (qPCR) was used to enumerate the HAdV and PRD1 present in the influent and effluent samples.

Polymerase Chain Reaction Primers and Standards

Human adenovirus were amplified using a previously published primer set (Heim et al., 2003). The PRD1 primer set was designed in this study, targeting a major capsid protein gene (GenBank no. M55567.1) using Primer3 software. A homology search was performed against the GenBank database sequence similarity using the BLAST program (<http://www.ncbi.nlm.nih.gov/BLAST/>). The analysis indicated that the designed primer pair was specific for the PRD1 bacteriophage. The forward primer used was PRD1 JSF1-AAACTTGACCCGAAAACGT (starting position 952) and reverse primer PRD1 JSR2-CGGTACG-GCTGGTGAAGTAT (starting position 1153).

The PCR-amplified products (i.e., cDNA/DNA) were purified using the QIAquick PCR purification kit (Qiagen) and cloned into the pGEM-T Easy Vector System (Promega), transferred into *E. coli* JM109 competent cells, and plated on LB agar ampicillin, isopropyl-β-D-thio-galactopyranoside, and X-Gal (5-bromo-4-chloro-3-indolyl-β-D-galactopyranoside) as recommended by the manufacturer. Plasmids were purified using a plasmid mini kit (Qiagen).

Purified plasmid DNA containing the PRD1 and HAdV inserts were quantified using a NanoDrop ND-1000 UV-Vis spectrophotometer (Thermo Fisher Scientific). Plasmid copies were calculated and a 10-fold serial dilution was prepared in DNase- and RNase-free water to a final concentration ranging from 10⁰ to 10⁶ copies μL⁻¹; aliquots were stored at -80°C until use. A 3-μL template from each dilution was used to prepare standard curves for qPCR.

Polymerase Chain Reaction Amplification

Quantitative PCR reactions were performed on Bio-Rad iQ5 (Bio-Rad Laboratories), using iQ SuperMix (Bio-Rad). Each 25-μL PCR reaction mixture contained 12.5 μL of SuperMix, 120 nmol L⁻¹ of each primer, and 3 μL of template DNA. Bovine serum albumin was added to each reaction mixture to a final concentration of 0.2 μg μL⁻¹ to relieve PCR inhibition (Kreader, 1996). For each PCR run, corresponding positive (i.e., target DNA) and negative (sterile water) controls were included. Thermal cycling conditions for PRD1 were: initial denaturation at 95°C for 5 min, followed by 40 cycles at 95°C for 10 s, 60°C for 10 s, and 72°C for 10 s, with a final extension of 5 min at 72°C. Thermal cycling conditions for HAdV were as outlined by Sidhu et al. (2010). A melt curve analysis was performed after the PCR run to differentiate between actual products and primer dimers, and to eliminate the possibility

of false-positive results. The melt curve was generated using 80 cycles of 10 s each, starting at 55°C and increasing in 0.5°C intervals to a final temperature of 95°C. The melting temperature for each amplicon was determined using the iQ5 software (Bio-Rad).

Polymerase Chain Reaction Reproducibility and Limit of Detection

The reproducibility of the qPCR was assessed by determining intra-assay repeatability and inter-assay reproducibility. The coefficient of variation (CV) was calculated using six dilutions (10⁶–10⁰ gene copies) of the PRD1 and HAdV plasmid DNA. Each dilution was tested in triplicate. The CV for evaluation of intra-assay repeatability was calculated based on the threshold cycle (C_T) value by testing the six dilutions six times in the same experiment. The CV for inter-assay reproducibility was calculated based on the C_T value of six dilutions on six different days. To determine the qPCR limit of the detection, known gene copies (i.e., 10⁶–10⁰) of the PRD1 and HAdV were tested with qPCR. The lowest number of gene copies that was detected consistently in replicate assays was considered as the qPCR limit of detection.

Enumeration of MS2 Bacteriophage

The enumeration of infectious MS2 was performed by means of a double-layer plaque assay according to methods of the International Organization for Standardization (1995). Briefly, working cultures of the host bacterium were inoculated in Tryptone–yeast extract–glucose broth and incubated at 36 ± 2°C in a water bath while shaking. When the optical density reached a cell density of approximately 10⁸ colony-forming units (cfu) mL⁻¹ (based on the data obtained in prior calibration measurements), the inoculum culture was taken from the incubator, immediately placed in melting ice to avoid the loss of F-pili by the cells, and used within 2 h. Semisolid Tryptone–yeast extract–glucose agar (ssTYGA) bottles were prepared in advance, and the melted agar was kept in a water bath at 45 ± 1°C. A solution of calcium chloride glucose, prepared with 3 ± 0.1 g of CaCl₂·2H₂O and 10 ± 0.1 g of glucose per 100 mL of DI water, was aseptically added. Supplemented ssTYGA in 2.5-mL aliquots were dispensed in capped culture tubes placed in a water bath until used. To each tube, 1 mL of the sample, or dilutions thereof, and 1 mL of the inoculum culture were added. Finally, tubes were carefully mixed and poured over the surface of Tryptone–yeast extract–glucose agar plates, distributed, and allowed to solidify. The plates were incubated upside-down at 36 ± 2°C for 18 ± 2 h, and the plaques were counted. Positive and negative controls were performed for each test series.

Even though qPCR was used to enumerate HAdV and PRD1, which does not indicate only infectious viruses but rather enumerates all gene copies present dead or alive, we can assume that for the short time period of the experiments, inactivation was minimal. As mentioned above, HAdV and PRD1 can survive for long periods in the subsurface. For the column tests using MS2, inactivation batch tests were performed to monitor the MS2 suspension, which remained stable throughout the duration of the experiments; however, inactivation may have been caused when the MS2 came into contact with the porous medium, resulting in an underestimation of MS2.

The 100-nm nanoparticles were enumerated using a Nikon Eclipse 8000 epifluorescence microscope with a 100× magnification objective (final magnification: 1000×). The microscope is equipped with an automatic stage that can be driven by the user such that the whole filtration area can be scanned. One hundred microliters of each sample was pipetted onto a filter area 4 mm in diameter, delineated with a fine black permanent marker, on a white Millipore Isopore membrane filter with a pore size of 0.05 μm. The filter was then placed on a metal holder (AES Chemunex, bioMérieux) with 10 μL of phosphate buffer solution to hold the filter in place. Scanning the whole 4-mm-diameter area delineated in black allowed a detection limit of one nanoparticle per 100-μL sample; however, the limit of quantification is higher due to random sampling error (intrinsic variability) and operational variability (four particles per filter if a relative precision of 50% is accepted [Stevenson et al., 2014]). This method of scanning the whole filter has been used by Knappett et al. (2008) to enumerate 1.5-μm carboxylated polystyrene particles, and Bales et al. (1997) used an epifluorescence microscope to count 100-nm carboxylated polystyrene particles (although not on the whole filtration area).

Data Analysis

Filtration Efficiency

The removal of the particles was quantified using colloid filtration theory, which calculates the collision efficiency, α (dimensionless), and can be determined from the following formulas: (Pieper et al., 1997)

$$\alpha = \frac{d \left\{ \left[1 - 2(\lambda/x) \ln(\text{RB}) \right]^2 - 1 \right\}}{6(1-\theta)\eta\lambda} \quad [1]$$

(Tufenkji and Elimelech, 2004)

$$\alpha = -\frac{2}{3} \frac{d}{(1-\theta)\eta x} \ln \left(\frac{C}{C_0} \right) \quad [2]$$

$$\alpha = \frac{2}{3} \frac{d\theta}{(1-\theta)\eta U} k_{a1} \quad [3]$$

where d is the mean grain size [L], λ is dispersivity [L], x is the length of the column [L], RB is relative mass recovery (dimensionless), θ is effective porosity (dimensionless), η is the single-collector efficiency (dimensionless), C/C_0 is the normalized concentration of the tracer at the breakthrough plateau [$M M^{-1}$], k_{a1} is an attachment rate coefficient [T^{-1}], explained in more detail below, and U is the Darcy velocity [$L T^{-1}$]. The value of RB was estimated by integrating the area under the breakthrough curve; U and λ are needed for the calculations of η and α . The measured flow rates were used for the U values, while λ was found by simulating the colloid breakthrough curves in HYDRUS-1D (Šimůnek et al., 2013). The η and α values were calculated based on the equations of Tufenkji and Elimelech (2004). A Hamaker constant of 7×10^{-21} J for PRD1 (Ryan et al., 1999) was used for both PRD1 and HAdV. A buoyant density of 1.085 g cm^{-3} was

used by Hijnen et al. (2005) to represent MS2 and *E. coli*, which covers the size range of our microorganisms.

Equation [1] is useful for colloid transport in field studies, whereas Eq. [2] is more appropriate for column studies. Both equations were used for comparison because Eq. [1] has the advantage of calculating α with the relative mass recovery (RB), which includes the attachment and detachment portion of the breakthrough curves. Equation [1] was applied to the observed data to calculate α because RB could be determined; however, for Eq. [2], the maximum value from the HYDRUS-1D modeled values was used for C/C_0 due to the fact that the observed values did not produce a steady C_{max} . Equation [3] was also used for comparison because it is calculated using the first attachment rate coefficient, k_{a1} , and is not dependent on steady breakthrough.

Transport Modeling

The software package HYDRUS-1D (Šimůnek et al., 2013) was used to model the breakthrough curves of the conservative tracer, NO_3^- , and two of the colloids tested: HAdV and PRD1. Advection–dispersion equations for colloid transport are implemented in a numerical model using a two-site attachment–detachment model and the following formulas (Schijven and Šimůnek, 2002):

$$\frac{\partial C}{\partial t} + \frac{\rho_b}{\theta} \frac{\partial S_1}{\partial t} + \frac{\rho_b}{\theta} \frac{\partial S_2}{\partial t} = \lambda \nu \frac{\partial^2 C}{\partial x^2} - \nu \frac{\partial C}{\partial x}$$

$$\frac{\rho_b}{\theta} \frac{\partial S_1}{\partial t} = k_{a1} C - \frac{\rho_b}{\theta} k_{d1} S_1 \quad [4]$$

$$\frac{\rho_b}{\theta} \frac{\partial S_2}{\partial t} = k_{a2} C - \frac{\rho_b}{\theta} k_{d2} S_2$$

where C is the concentration of the tracer [$M L^{-3}$], t is time [T], ρ_b [$M L^{-3}$] is dry bulk density, θ (dimensionless) is effective porosity, S_1 and S_2 are the concentrations of sorbed particles at the first and second kinetic sorption sites [$M M^{-1}$], λ is dispersivity [L], ν is pore water velocity [$L T^{-1}$], x is distance along the flow path [L], and k_{a1} and k_{a2} are attachment rate coefficients [T^{-1}] while k_{d1} and k_{d2} are detachment rate coefficients [T^{-1}] at the first and second kinetic sorption sites. To determine the bias, the observed breakthrough curve was compared with the modeled curve by finding the logarithm of the difference of the averages as well as of the 95th percentiles. Inactivation was not modeled because, for the short duration of our experiments, inactivation was not an issue for HAdV and PRD1.

Results and Discussion

Porous Media and Colloid Characterization

Zeta potential (ZP) measurements were done for all colloids in 10 mmol L^{-1} NaCl, pH 8.0 ± 0.2 , and the ZP was found to be -15.0 ± 2.0 mV for the HAdV used in this study. Wong et al. (2012) measured a ZP of approximately (read from a graph) -24 mV for HAdV Serotype 2 in 10 mmol L^{-1} NaCl at pH 8. Pang et al. (2014) measured ZPs of -24 and -27 mV for purified HAdV Type 41 and MS2, respectively, in 2 mmol L^{-1} NaCl at pH 7. The MS2 used in this study had a ZP of -16.6 ± 1.3 mV, which was most like the ZP of the HAdV, and PRD1 had a ZP

of -7.8 ± 2.6 mV. The ZP of PRD1 was measured to be -9.8 mV by Mesquita et al. (2010).

In our study, the 100-nm carboxylated polystyrene nanoparticles had a ZP of -70.4 ± 2.8 mV compared with approximately -42 mV (read from a graph) measured by Pang et al. (2009) for 20-nm carboxylated polystyrene particles (Bangs Laboratories, Inc.) in 1 mmol L^{-1} NaCl at pH 8 and -37 mV for 70-nm carboxylated silica particles (Micromod Partikeltechnologie GmbH) in 2 mmol L^{-1} NaCl at pH 7 (Pang et al., 2014). The studies using nanoparticles chosen for comparison differ from our study by similarity in particle material (Pang et al., 2009) and size (Pang et al., 2014), but measurements of ZP can also vary depending on the ionic strength and pH, as well as the measuring instrument used and the colloid manufacturer. In the two studies mentioned for comparison, the measuring instrument was the same as that used in our study, although the colloid manufacturers differed as did the solution chemistries.

Our measurements of ZP were generally less negative (except for the 100-nm particles) than the measurements found in comparable studies; however, the measurements relative to each other (i.e., nanoparticles were most negative, PRD1 least negative) were consistent with other studies. The ZP of the porous medium used in our study was -38.7 ± 0.9 mV.

Column Tests

Table 1 lists the test conditions and measured parameters for each of the seven column test runs. Log-removal (\log_{10} of C_{max}/C_0), which is not dependent on detachment because it is only looking at the initial attachment phase, was highest for the 100-nm particles and MS2. The log-removal of PRD1 was slightly higher than that of HAdV. Run 1 for the HAdV had the least log-removal, even though 0.5 mmol L^{-1} Ca^{2+} was added to the solution, which usually causes more colloidal removal (Bales et al., 1991; Sadeghi et al., 2013). Our system was dominated by calcite, and it may be that adding a small amount of Ca^{2+} produced a negligible effect.

No clumping of the 100-nm particles was observed under the microscope, but the number of nanoparticles that did break through was below the limit of quantification. The 100-nm particles, being the largest of the colloids tested, may have been subject to straining, although this seems unlikely due to the small ratio of colloid diameter to mean grain size (<0.0017) (Bradford et al., 2002). An exception has been hypothesized by Tufenkji et al. (2004) that angular porous media, such as the material used in this study, can result in irregular packing, which in turn can cause much smaller pore spaces than those predicted using the mean grain size. Nevertheless, if straining were the only removal

mechanism, then the much smaller MS2 would have broken through significantly more than the 100-nm particles, which was not the case in our study. This is difficult to confirm without quantifying the surface inactivation rate of MS2 that came into contact with the porous medium.

Filtration Removal of Colloids

Colloid filtration theory was used to compare the removal of HAdV to that of PRD1. The contact efficiency (the ratio of the rate at which colloids collide with the porous medium to the rate at which colloids flow), η , was 0.19 for both PRD1 tests and 0.14 for all three HAdV tests (Table 2). This means that, in theory, there were more collisions of PRD1 with the granular limestone. The collision efficiency (the number of successful contacts that result in attachment divided by the number of collisions) was calculated using three different equations: for field tests (α_1), for column tests (α_2), and using the first attachment rate coefficient (α_3). The results (Table 2) show that α_1 was lower for the PRD1 tests than for the HAdV tests, demonstrating less removal by attachment to the porous medium or more detachment of PRD1. Because α_1 is dependent on the relative mass recovery (RB), it also reflects the higher detachment of PRD1 under high-pH conditions relative to HAdV. Additionally, Run 3 was run for twice as long as Run 2 and should have more detachment; this is reflected in the relatively lower α_1 values for Run 3. Run 1, which was only run for the attachment portion of the experiment, had the highest α_1 value.

The values of α_2 and α_3 are higher than the α_1 values (with the exception of Run 1 [no detachment] and α_3 for HAdV, Run 3) because detachment is not taken into account, hence the higher removal. Similar to the α_1 values, the α_2 and α_3 values are higher for HAdV than for PRD1. This further supports the claim that there was less removal of PRD1. In contrast, Fig. 1B appears to show that there was less removal of HAdV by an order of magnitude. This ambiguity infers that PRD1 may not be a perfect surrogate for HAdV but the best of the surrogates tested. Even though detachment was not taken into account, the values of α_2 and α_3 are lower for Run 3. Thus, it appears that not only did detachment cause less removal for Run 3 but there was also less attachment. The averages and standard deviations of the three collision coefficients are shown in Table 2 and demonstrate the high variability of the calculated α values.

The values of η and α were not calculated for MS2 or the 100-nm particles because the breakthrough was almost entirely below the limit of quantification for these colloids.

Table 2. Comparison of collision coefficients in experiments using human adenovirus (HAdV) and bacteriophage PRD1: observed relative mass recovery including detachment (RB), single collector factor (η), collision coefficient for field including detachment (α_1), collision coefficient for column tests (α_2), collision coefficient calculated from the first attachment rate coefficient k_{a1} (α_3), average of three collision coefficients (α_{avg}), and standard deviation of the collision coefficients (SD).

Tracer	Run	RB	η	α_1	α_2	α_3	α_{avg}	SD
HAdV	1	2.63×10^{-4}	0.14	0.154	0.133	0.008	0.099	0.079
HAdV	2	7.22×10^{-4} †	0.14	0.138†	0.165	0.180	0.161	0.021
HAdV	3	1.49×10^{-2} †	0.14	0.078†	0.177	0.054	0.103	0.065
PRD1	2	8.79×10^{-3} †	0.19	0.063†	0.136	0.154	0.118	0.048
PRD1	3	7.40×10^{-1} †	0.19	0.004†	0.125	0.038	0.056	0.062

† Includes detachment.

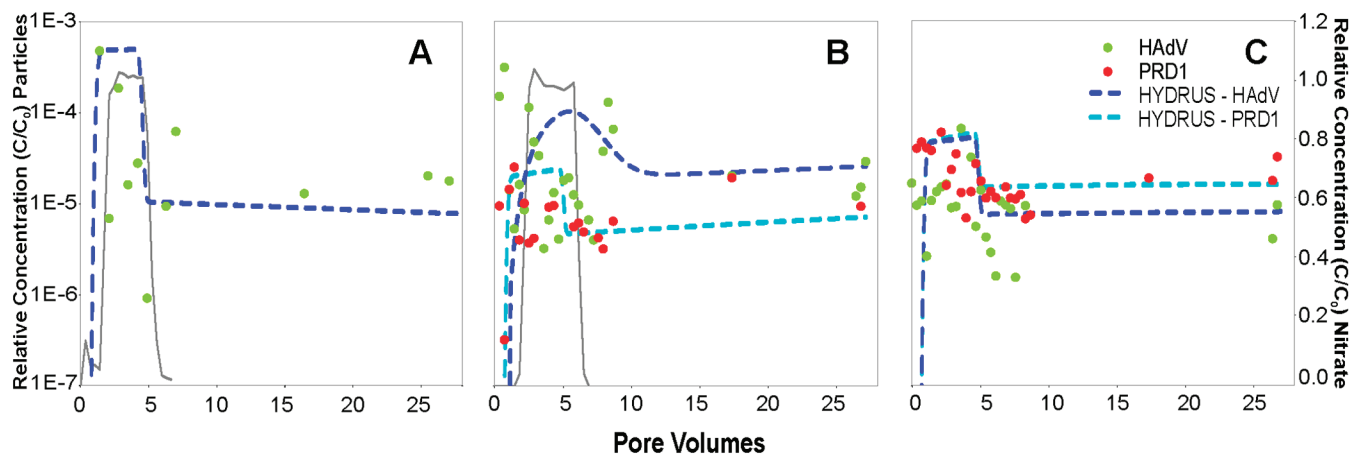


Fig. 1. Observed breakthrough curves of human adenovirus (HAdV) and bacteriophage PRD1 for (A) Test Run 1, (B) Test Run 2, and (C) Test Run 3 and simulation results of modeling performed in HYDRUS-1D. Nitrate breakthrough curves are shown in gray for Runs 1 and 2, right y axis.

Transport of Colloids

Modeling

To characterize the transport of HAdV and the surrogates in the porous medium, we attempted to model the breakthrough curves using HYDRUS-1D. Our intention was to model the NO_3^- breakthrough curves to determine the flow rate and dispersivity; however, this turned out to be a challenge. Therefore, different flow rates and dispersivities were used for the conservative tracer and the colloids, as can be seen in Table 3.

The pore water velocity (ν) and dispersivity (λ) of the conservative tracer and the colloids were calculated separately because the granular limestone was quite diverse in shape and would not result in a uniform packing. In some heterogeneous material, size exclusion of the colloids can play a role and colloidal transport can be controlled by advective processes, with less λ than solute tracers and higher ν (Pang et al., 2005). This effect was seen in our material where the conservative tracer (NO_3^-) had ν values of 0.10 to 0.11 cm min^{-1} and the colloids 0.13 to 0.15 cm min^{-1} . The λ of the NO_3^- tracer was modeled to be 0.09 to 0.15 cm and all the colloids had a λ of 0.08 cm. Because the NO_3^- tests were analyzed outside of the quarantine area used for pathogenic microorganisms, it was necessary to run the conservative tracer test ahead of the test using the pathogenic viruses. Consequently, it is possible that the tests were run slightly slower or faster, but this was considered negligible because the sample volumes were consistent. The breakthrough of the viruses preceded the breakthrough of the conservative tracer, demonstrating preferential flow due to the heterogeneous nature of the material and packing. This is known as *velocity enhancement* (Pang et al., 2005), when the preferential flow path acts as a high-speed motorway for the colloids while the solute slowly disperses into the smaller pore spaces.

The data from the colloid column experiments was scattered, a challenge when quantifying low-concentration samples, which can have relatively high intrinsic variability, and almost impossible to model. Only the constant IS portion of the breakthrough data was modeled. Figure 1 shows the breakthrough curves for all the HAdV and PRD1 tests. PRD1 appears to attach and detach more than HAdV, and the attachment and detachment values are the same or slightly higher for PRD1, except for the secondary attachment and detachment coefficients for Run 2 (Table 3).

The R^2 values for the HAdV tests ranged from 0.16 to 0.26, while the R^2 value for both PRD1 tests was 0.03, which signifies that there was almost no fit at all. Therefore, as an alternative method of comparison, the logarithms of the differences of the averages and 95th percentiles were calculated and are displayed in Table 3.

There was minimal to no breakthrough for column tests done with MS2 and the 100-nm particles; breakthrough was below the limit of quantification. A lower count of MS2 might be expected due to the fact that plaque-forming analysis generally enumerates fewer microorganisms than qPCR but, on the contrary, Pang et al. (2014) found that MS2 (enumerated by plaque-forming analysis) exhibited higher breakthrough in saturated sand columns than HAdV (enumerated by qPCR). Even so, it has been shown that media containing Fe oxides (e.g., pyrite, hematite, and goethite) can cause surface inactivation due to the strong electrostatic interaction with negatively charged viruses and is more notable in the inactivation of MS2 relative to PRD1 (Ryan et al., 2002). The breakthrough of the nanoparticles was also quite low, probably because the nanoparticles had a very negative surface charge (approximately -70 mV), even though the limit of quantification for enumerating the nanoparticles was very low (four particles per filter based on Poisson distribution; Stevenson et al., 2014).

Due to the low breakthrough, we did not attempt to model the breakthrough curves for MS2 or the 100-nm particles. Interestingly, MS2 is usually used as a conservative surrogate, although in our study it was the least conservative, along with the 100-nm particles. The fact that MS2 and the 100-nm particles broke through minimally demonstrates that straining was not a removal mechanism and that the size and structure of PRD1 influenced attachment more than the surface charge.

Detachment of Viruses

Attachment of viruses was very reversible. Column elution tests were done by alternating injection of 1.2 pore volumes of DI water and 50 mmol L^{-1} glycine (1.5% beef extract) at pH 10. Figure 2 shows how the HAdV and PRD1 colloids attach and become a constant source of contamination that can be aggravated by changes in the chemistry of the influent water, i.e., high IS and pH. Interestingly, PRD1 detaches much more than HAdV and is less negatively charged than HAdV, hence

Table 3. Summary of calculated and modeled parameters using HYDRUS-1D: pore water velocity (ν), dispersivity (λ), peak concentration (C_{max}), injection concentration (C_0), attachment rate coefficients at first and second sorption sites (k_{a1} and k_{a2}), detachment rate coefficients at first and second sorption sites (k_{d1} and k_{d2}), and log-differences of observed to simulated data (average and 95th percentile).

Tracer	Run	ν cm min ⁻¹	λ cm	C_{max}/C_0	$\log_{10}(C_{max}/C_0)$	k_{a1}	k_{d1}	k_{a2}	k_{d2}	R^2	Observed (obs)		Simulated (sim)		log(obs/sim)		
											Avg.	95%	Avg.	95%	Avg.	95%	
NO ₃ ⁻	1	0.10	0.15	1.00 × 10 ⁰	0	-	-	-	-	0.99	-	-	-	-	-	-	-
NO ₃ ⁻	2	0.11	0.09	1.00 × 10 ⁰	0	-	-	-	-	0.95	-	-	-	-	-	-	-
HAdV	1	0.13	0.08	4.98 × 10 ⁻⁴	-3.30	0.006	0.0003	0.1	0	0.26	5.72 × 10 ⁻⁵	2.80 × 10 ⁻⁴	6.37 × 10 ⁻⁵	4.94 × 10 ⁻⁴	-0.05	-0.25	
HAdV	2	0.15	0.08	1.02 × 10 ⁻⁴	-3.99	0.15	0.00009	0.12	0.05	0.19	4.00 × 10 ⁻⁵	1.45 × 10 ⁻⁴	3.30 × 10 ⁻⁵	9.59 × 10 ⁻⁵	0.08	0.18	
HAdV	3	0.15	0.08	5.24 × 10 ⁻⁵	-4.28	0.045	0.0003	0.12	0	0.16	1.10 × 10 ⁻⁵	2.76 × 10 ⁻⁵	9.81 × 10 ⁻⁶	1.67 × 10 ⁻⁵	0.05	0.22	
PRD1	2	0.15	0.08	2.38 × 10 ⁻⁵	-4.62	0.18	0.0001	0.0001	0.0001	0.03	5.21 × 10 ⁻⁶	1.75 × 10 ⁻⁵	7.91 × 10 ⁻⁶	2.24 × 10 ⁻⁵	-0.18	-0.11	
PRD1	3	0.15	0.08	5.93 × 10 ⁻⁵	-4.23	0.045	0.0006	0.12	0	0.03	2.11 × 10 ⁻⁵	4.55 × 10 ⁻⁵	1.66 × 10 ⁻⁵	2.05 × 10 ⁻⁵	0.10	0.35	

is not as strongly bonded to patches of positive charge present on the surface of the aquifer material. Relative to PRD1, HAdV detaches minimally (see Fig. 2) after a cycle of DI water and glycine, which is apparent in the lower relative mass recovery of HAdV. Both tests show that the relative mass recovery of HAdV is an order of magnitude lower than that of PRD1 (Table 2). For Run 2, HAdV and PRD1 had a lower relative mass recovery compared with the other test runs because this test had a much shorter duration: 54 compared with 109 pore volumes.

During the detachment tests, two peaks occurred (Fig. 2), at 31 and 34 pore volumes for the first run and at 87 and 89 pore volumes for the second run. The beginning of injection of the two DI water cycles was approximately two pore volumes apart, and the two detachment peaks are separated by two to three pore volumes. The second peak, for both test runs, coincided with a significant amount of brown material observed in the effluent samples. There was no suspended fine material observed in the samples taken during the first peak. The release of aquifer material during the second peak indicates that the high-IS water followed by DI water caused the release of viruses with, and perhaps attached to, the aquifer material.

A study by Bradford and Kim (2010) looked at the effect of different cycles of DI water and high-IS water on the removal of clay. They found that the highest clay removal occurred during the DI phase and that the most clay was removed when the highest IS was injected just before the DI. They used 0.1, 1, 10, and 100 mmol L⁻¹ NaCl, as well as 100 mmol L⁻¹ CaCl₂. Tosco et al. (2009) also found that colloids were released during the DI water phase of an experiment. They injected carboxylated latex microspheres into sand columns with different IS solutions (1–300 mmol L⁻¹ NaCl at pH 6.8), followed by a flushing of DI water, to test the effect of IS on the transport and release of colloids. They found the highest release of colloids during the DI phase after high-IS (30–300 mmol L⁻¹) experiments, and they observed that no particles were released after a solution with an IS of 1 to 10 mmol L⁻¹ followed by DI water.

Whereas in the studies by Bradford and Kim (2010) and Tosco et al. (2009) the release happened during the DI water injection, our system exhibited a delayed response, which may have been due to the different porous media used. The two studies mentioned used columns of sand, while in our study the material in the column was 63% calcite. The naturally occurring Ca²⁺ added complexity to chemical changes in our system. Our detachment experiments show that strongly attached HAdV could be a constant source of contamination in a limestone aquifer and could cause a constant slow release of viruses and a large release when aggravated by changes in groundwater chemistry.

Conclusions

Managed aquifer recharge is becoming a popular initial treatment option for drinking water due to its efficiency and low costs; however, injecting stormwater runoff into the subsurface can introduce pathogenic microorganisms into the groundwater. Our study considered the transport of HAdV in the subsurface and compared the transport and removal to various surrogates that are diverse in size, morphology, and

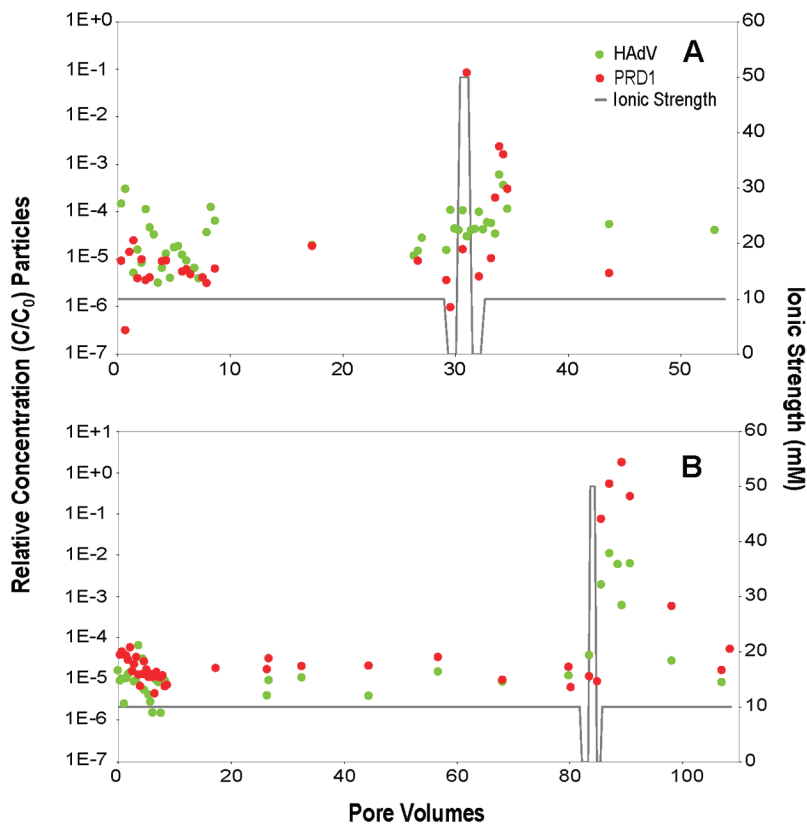


Fig. 2. Detachment curves for human adenovirus (HAdV) and bacteriophage PRD1 for (A) Test Run 2 and (B) Test Run 3. Ionic strength (gray curve) is plotted relative to the right y axis.

surface charge. Of the three surrogates tested, PRD1 was the best surrogate for HAdV. MS2 and the 100-nm carboxylated polystyrene particles showed minimal breakthrough and did not mimic the transport and removal of HAdV. We looked at the dominant mechanisms of removal and the possible colloid characteristics that could influence this. With MS2 and the 100-nm particles, we tested the possibility of straining being a mechanism. If straining were an issue, then the MS2 would have broken through more than the other three colloids, which it did not. Because MS2 was not transported like HAdV, we can also conclude that surface charge is not a dominant factor. PRD1 has a similar size, shape, and structure to HAdV and was the best surrogate for aquifer material dominated by calcite, but it could not model the magnitude of detachment of HAdV under high-IS, high-pH conditions. Therefore, size, morphology, and perhaps the surface macromolecules are the dominant characteristics that control the fate and transport of HAdV in fine granular limestone material. This study demonstrates the importance of testing the surrogates and comparing them with the real pathogenic microorganisms in laboratory tests using the aquifer medium from the site under consideration. Implications of this study could influence how field tests using bacteriophages and nanoparticles are interpreted.

Acknowledgments

This work was supported by the Austrian Science Fund (FWF) as part of the DK-Plus 1219-N22 (Vienna Doctoral Program on Water Resource Systems). Additional support came from the project Groundwater Resource Systems Vienna (GWRS-Vienna), funded by Vienna Waterworks. We would like to thank Liping Pang (ESR New Zealand), Rupak Aryal (University of Queensland), Ronald Zirbs (University of Natural Resources and Life Sciences, Vienna), and Susanne Laumann (University of Vienna) for their help and advice. The research work was also supported by the CSIRO Water for a Healthy

Country Flagship Program (Australia). We acknowledge the support of Karen Barry (CSIRO) for providing the aquifer material used in this study. This study is a joint publication of the Interuniversity Cooperation Centre Water & Health (www.waterandhealth.at).

References

- Ahmed, W., A. Goonetilleke, and T. Gardner. 2010. Human and bovine adenoviruses for the detection of source-specific fecal pollution in coastal waters in Australia. *Water Res.* 44:4662–4673. doi:10.1016/j.watres.2010.05.017
- Albinana-Gimenez, N., P. Clemente-Casares, S. Bofill-Mas, A. Hundsda, F. Ribas, and R. Girones. 2006. Distribution of human polyomaviruses, adenoviruses, and hepatitis E virus in the environment and in a drinking-water treatment plant. *Environ. Sci. Technol.* 40:7416–7422. doi:10.1021/es060343i
- Bales, R.C., S.R. Hinkle, T.W. Kroeger, K. Stocking, and C.P. Gerba. 1991. Bacteriophage adsorption during transport through porous-media: Chemical perturbations and reversibility. *Environ. Sci. Technol.* 25:2088–2095. doi:10.1021/es00024a016
- Bales, R.C., S.M. Li, T.C.J. Yeh, M.E. Lenczewski, and C.P. Gerba. 1997. Bacteriophage and microsphere transport in saturated porous media: Forced-gradient experiment at Borden, Ontario. *Water Resour. Res.* 33:639–648. doi:10.1029/97WR00025
- Blanc, R., and A. Nasser. 1996. Effect of effluent quality and temperature on the persistence of viruses in soil. *Water Sci. Technol.* 33:237–242. doi:10.1016/0273-1223(96)00425-8
- Bofill-Mas, S., N. Albinana-Gimenez, P. Clemente-Casares, A. Hundsda, J. Rodriguez-Manzano, A. Allard, et al. 2006. Quantification and stability of human adenoviruses and polyomavirus JCPyV in wastewater matrices. *Appl. Environ. Microbiol.* 72:7894–7896. doi:10.1128/AEM.00965-06
- Bradbury, K.R., M.A. Borchardt, M. Gotkowitz, S.K. Spencer, J. Zhu, and R.J. Hunt. 2013. Source and transport of human enteric viruses in deep municipal water supply wells. *Environ. Sci. Technol.* 47:4096–4103. doi:10.1021/es400509b
- Bradford, S.A., and H. Kim. 2010. Implications of cation exchange on clay release and colloid-facilitated transport in porous media. *J. Environ. Qual.* 39:2040–2046. doi:10.2134/jeq2010.0156
- Bradford, S.A., S.R. Yates, M. Bettahar, and J. Šimůnek. 2002. Physical factors affecting the transport and fate of colloids in saturated porous media. *Water Resour. Res.* 38(12):1327. doi:10.1029/2002wr001340

- Calgua, B., A. Carratala, L. Guerrero-Latorre, A.D. Correa, T. Kohn, R. Sommer, and R. Girones. 2014. UVC inactivation of dsDNA and ssRNA viruses in water: UV fluences and a qPCR-based approach to evaluate decay on viral infectivity. *Food Environ. Virol.* 6:260–268. doi:10.1007/s12560-014-9157-1
- Corsi, S.R., M.A. Borchart, S.K. Spencer, P.E. Hughes, and A.K. Baldwin. 2014. Human and bovine viruses in the Milwaukee River watershed: Hydrologically relevant representation and relations with environmental variables. *Sci. Total Environ.* 490:849–860. doi:10.1016/j.scitotenv.2014.05.072
- Davies, C.M., M.R. Logan, V.J. Rothwell, M. Krogh, C.M. Ferguson, K. Charles, et al. 2006. Soil inactivation of DNA viruses in septic seepage. *J. Appl. Microbiol.* 100:365–374. doi:10.1111/j.1365-2672.2005.02777.x
- Dillon, P., D. Page, J. Vanderzalm, P. Pavelic, S. Toze, E. Bekele, et al. 2008. A critical evaluation of combined engineered and aquifer treatment systems in water recycling. *Water Sci. Technol.* 57:753–762. doi:10.2166/wst.2008.168
- Futch, J.C., D.W. Griffin, and E.K. Lipp. 2010. Human enteric viruses in groundwater indicate offshore transport of human sewage to coral reefs of the Upper Florida Keys. *Environ. Microbiol.* 12:964–974. doi:10.1111/j.1462-2920.2010.02141.x
- Harvey, R.W., and J.N. Ryan. 2004. Use of PRD1 bacteriophage in groundwater viral transport, inactivation, and attachment studies. *FEMS Microbiol. Ecol.* 49:3–16. doi:10.1016/j.femsec.2003.09.015
- Heim, A., C. Ebner, G. Harste, and P. Pring-Akerblom. 2003. Rapid and quantitative detection of human adenovirus DNA by real-time PCR. *J. Med. Virol.* 70:228–239. doi:10.1002/jmv.10382
- Hijnen, W.A.M., A.J. Brouwer-Hanzens, K.J. Charles, and G.J. Medema. 2005. Transport of MS2 phage, *Escherichia coli*, *Clostridium perfringens*, *Cryptosporidium parvum* and *Giardia intestinalis* in a gravel and a sandy soil. *Environ. Sci. Technol.* 39:7860–7868. doi:10.1021/es050427b
- International Organization for Standardization. 1995. Water quality: Detection and enumeration of bacteriophages (ISO 10705-1). ISO, Geneva.
- Knappett, P.S.K., M.B. Emelko, J. Zhuang, and L.D. McKay. 2008. Transport and retention of a bacteriophage and microspheres in saturated, angular porous media: Effects of ionic strength and grain size. *Water Res.* 42:4368–4378. doi:10.1016/j.watres.2008.07.041
- Kokkinos, P., V.I. Syngouna, M.A. Tselepi, M. Bellou, C.V. Chrysikopoulos, and A. Vantarakis. 2015. Transport of human adenoviruses in water saturated laboratory columns. *Food Environ. Virol.* 7:122–131. doi:10.1007/s12560-014-9179-8
- Kreader, C.A. 1996. Relief of amplification inhibition in PCR with bovine serum albumin or T4 gene 32 protein. *Appl. Environ. Microbiol.* 62:1102–1106.
- Luong, D.T., and R. Sprik. 2013. Streaming potential and electroosmosis measurements to characterize porous materials. *ISRN Geophysics* 2013:496352. doi:10.1155/2013/496352
- Mesquita, M.M., J. Stimson, G.T. Chae, N. Tufenkji, C.J. Ptacek, D.W. Blowes, and M.B. Emelko. 2010. Optimal preparation and purification of PRD1-like bacteriophages for use in environmental fate and transport studies. *Water Res.* 44:1114–1125. doi:10.1016/j.watres.2009.11.017
- Mondal, P.K., and B.E. Sleep. 2013. Virus and virus-sized microsphere transport in a dolomite rock fracture. *Water Resour. Res.* 49:808–824. doi:10.1002/wrcr.20086
- Pang, L., U. Nowostawska, J.N. Ryan, W.M. Williamson, G. Walshe, and K.A. Hunter. 2009. Modifying the surface charge of pathogen-sized microspheres for studying pathogen transport in groundwater. *J. Environ. Qual.* 38:2210–2217. doi:10.2134/jeq2008.0451
- Pang, L.P., M. Close, M. Goltz, M. Noonan, and L. Sinton. 2005. Filtration and transport of *Bacillus subtilis* spores and the F-RNA phage MS2 in a coarse alluvial gravel aquifer: Implications in the estimation of setback distances. *J. Contam. Hydrol.* 77:165–194. doi:10.1016/j.jconhyd.2004.12.006
- Pang, L.P., K. Farkas, G. Bennett, A. Varsani, R. Easingwood, R. Tilley, et al. 2014. Mimicking filtration and transport of rotavirus and adenovirus in sand media using DNA-labeled, protein-coated silica nanoparticles. *Water Res.* 62:167–179. doi:10.1016/j.watres.2014.05.055
- Paul, J.H., J.B. Rose, J. Brown, E.A. Shinn, S. Miller, and S.R. Farrar. 1995. Viral tracer studies indicate contamination of marine waters by sewage disposal practices in Key Largo, Florida. *Appl. Environ. Microbiol.* 61:2230–2234.
- Paul, J.H., J.B. Rose, S.C. Jiang, X.T. Zhou, P. Cochran, C. Kellogg, et al. 1997. Evidence for groundwater and surface marine water contamination by waste disposal wells in the Florida Keys. *Water Res.* 31:1448–1454. doi:10.1016/S0043-1354(96)00374-0
- Pieper, A.P., J.N. Ryan, R.W. Harvey, G.L. Amy, T.H. Illangasekare, and D.W. Metge. 1997. Transport and recovery of bacteriophage PRD1 in a sand and gravel aquifer: Effect of sewage-derived organic matter. *Environ. Sci. Technol.* 31:1163–1170. doi:10.1021/es960670y
- Redman, J.A., S.B. Grant, T.M. Olson, M.E. Hardy, and M.K. Estes. 1997. Filtration of recombinant Norwalk virus particles and bacteriophage MS2 in quartz sand: Importance of electrostatic interactions. *Environ. Sci. Technol.* 31:3378–3383. doi:10.1021/es961071u
- Rodriguez, R.A., P.M. Gundy, and C.P. Gerba. 2008. Comparison of BGM and PLC/PRC/5 cell lines for total culturable viral assay of treated sewage. *Appl. Environ. Microbiol.* 74:2583–2587. doi:10.1128/AEM.00626-07
- Ryan, J.N., M. Elimelech, R.A. Ard, R.W. Harvey, and P.R. Johnson. 1999. Bacteriophage PRD1 and silica colloid transport and recovery in an iron oxide-coated sand aquifer. *Environ. Sci. Technol.* 33:63–73. doi:10.1021/es980350+
- Ryan, J.N., R.W. Harvey, D. Metge, M. Elimelech, T. Navigato, and A.P. Pieper. 2002. Field and laboratory investigations of inactivation of viruses (PRD1 and MS2) attached to iron oxide-coated quartz sand. *Environ. Sci. Technol.* 36:2403–2413. doi:10.1021/es011285y
- Sadeghi, G., T. Behrends, J.F. Schijven, and S.M. Hassanizadeh. 2013. Effect of dissolved calcium on the removal of bacteriophage PRD1 during soil passage: The role of double-layer interactions. *J. Contam. Hydrol.* 144:78–87. doi:10.1016/j.jconhyd.2012.10.006
- Schijven, J.F., H.A.M. de Bruin, S.M. Hassanizadeh, and A.M.D. Husman. 2003. Bacteriophages and clostridium spores as indicator organisms for removal of pathogens by passage through saturated dune sand. *Water Res.* 37:2186–2194. doi:10.1016/S0043-1354(02)00627-9
- Schijven, J.F., and J. Šimůnek. 2002. Kinetic modeling of virus transport at the field scale. *J. Contam. Hydrol.* 55:113–135. doi:10.1016/S0169-7722(01)00188-7
- Sidhu, J.P., L. Hodggers, W. Ahmed, M.N. Chong, and S. Toze. 2012. Prevalence of human pathogens and indicators in stormwater runoff in Brisbane, Australia. *Water Res.* 46:6652–6660. doi:10.1016/j.watres.2012.03.012
- Sidhu, J.P.S., S. Toze, L. Hodggers, M. Shackleton, K. Barry, D. Page, and P. Dillon. 2010. Pathogen inactivation during passage of stormwater through a constructed reedbed and aquifer transfer, storage and recovery. *Water Sci. Technol.* 62:1190–1197. doi:10.2166/wst.2010.398
- Šimůnek, J., D. Jacques, G. Langergraber, S.A. Bradford, M. Sejna, and M.T. van Genuchten. 2013. Numerical modeling of contaminant transport using HYDRUS and its specialized modules. *J. Indian Inst. Sci* 93:265–284.
- Sinton, L.W., R.K. Finlay, L. Pang, and D.M. Scott. 1997. Transport of bacteria and bacteriophages in irrigated effluent into and through an alluvial gravel aquifer. *Water Air Soil Pollut.* 98:17–42. doi:10.1007/Bf02128648
- Sobsey, M.D., R.M. Hall, and R.L. Hazard. 1995. Comparative reductions of hepatitis A virus, enteroviruses and coliphage MS2 in miniature soil columns. *Water Sci. Technol.* 31:203–209. doi:10.1016/0273-1223(95)00267-Q
- Stevenson, M.E., A.P. Blaschke, S. Schauer, M. Zessner, R. Sommer, A.H. Farnleitner, and A.K.T. Kirschner. 2014. Enumerating microorganism surrogates for groundwater transport studies using solid-phase cytometry. *Water Air Soil Pollut.* 225:1827. doi:10.1007/S11270-013-1827-3
- Stevenson, M.E., A.P. Blaschke, S. Toze, J.P. Sidhu, W. Ahmed, I.H. van Driezum, et al. 2015. Biotin- and glycoprotein-coated microspheres as surrogates for studying filtration removal of *Cryptosporidium parvum* in granular limestone aquifer media. *Appl. Environ. Microbiol.* 81:4277–4283. doi:10.1128/AEM.00885-15
- Tosco, T., A. Tiraferri, and R. Sethi. 2009. Ionic strength dependent transport of microparticles in saturated porous media: Modeling mobilization and immobilization phenomena under transient chemical conditions. *Environ. Sci. Technol.* 43:4425–4431. doi:10.1021/es900245d
- Tufenkji, N., and M. Elimelech. 2004. Correlation equation for predicting single-collector efficiency in physicochemical filtration in saturated porous media. *Environ. Sci. Technol.* 38:529–536. doi:10.1021/es034049r
- Tufenkji, N., G.F. Miller, J.N. Ryan, R.W. Harvey, and M. Elimelech. 2004. Transport of *Cryptosporidium* oocysts in porous media: Role of straining and physicochemical filtration. *Environ. Sci. Technol.* 38:5932–5938. doi:10.1021/es049789u
- Wong, K., D. Bouchard, and M. Molina. 2014. Relative transport of human adenovirus and MS2 in porous media. *Colloids Surf. B* 122:778–784. doi:10.1016/j.colsurfb.2014.08.020
- Wong, K., B. Mukherjee, A.M. Kahler, R. Zepp, and M. Molina. 2012. Influence of inorganic ions on aggregation and adsorption behaviors of human adenovirus. *Environ. Sci. Technol.* 46:11145–11153. doi:10.1021/es3028764